Available online at www.sciencedirect.com

ScienceDirect

Virology 374 (2008) 186–197

VIROLOGY

www.elsevier.com/locate/yviro

A novel rodent papillomavirus isolated from anogenital lesions in its natural host

Julia Nafz [a,*], Kai Schäfer [a], Su Feng Chen, Ignacio G. Bravo [b,c], Myriam Ibberson [a], Ingo Nindl [a,d], Eggert Stockfleth [d], Frank Rösl [a,*]

[a] *Applied Tumorvirology, Division Viral Transformation Mechanisms, German Cancer Research Center, Heidelberg, Germany*
[b] *Applied Tumorvirology, Division Genome Modification and Carcinogenesis, German Cancer Research Center, Heidelberg, Germany*
[c] *Experimental Molecular Evolution, Institute for Evolution and Biodiversity, University of Münster, Germany*
[d] *Department of Dermatology, Charité, Skin Cancer Center Charité, University Hospital, Berlin, Germany*

Received 12 October 2007; returned to author for revision 19 November 2007; accepted 7 December 2007
Available online 29 January 2008

Abstract

In the present work we describe both the prevalence and the histopathologic features of a novel papillomavirus (referred as McPV2) that naturally infects the rodent *Mastomys coucha*. Viral DNA could be isolated not only from anogenital wart-like lesions but also from healthy tissues (e.g. liver, kidney, spleen and intestine) without apparent signs of infection. Our finding of a second papillomavirus infecting *M. coucha*, phylogenetically very distant from the previously known MnPV, reinforces the growing view of warm-blooded vertebrates as being hosts for a number of different papilloma virus types that are not necessarily closely related. The histological descriptions of McPV2-associated anogenital lesions provided here, together with earlier knowledge on MnPV-associated skin carcinogenesis, define *M. coucha* as an excellent system where the link between infection towards malignancy can be studied in molecular, histochemical and immunological terms in immunocompetent animals. The availability of such an *in vivo* model also offers the unique opportunity to address defined questions about prophylactic and therapeutic strategies against different papillomavirus infections in their natural host. To date, McPV2 is the first rodent papillomavirus found in anogenital lesions.

Keywords: *Mastomys coucha*; MnPV; Skin carcinogenesis; Condyloma

Introduction

Extensive studies have established a causal relationship between high risk human papillomaviruses (HPVs) and the development of cervical cancer (for review, see Zur Hausen, 2002). Additionally, particular cutaneous HPVs have transforming properties *in vivo* (for review, see Akgül et al., 2006) and are involved in skin carcinogenesis of immunosuppressed and/or genetically predisposed patients (for review, see Majewski and Jablonska, 2006; Nindl et al., 2007). However, the pathogenic nature of host–virus interactions of most papillomaviruses (PVs) is still inadequately understood, mainly hampered by the absence of suitable model systems (Woodman et al., 2007). The dependency on epithelial differentiation and their almost strict species specificity are the main hindrances for the study of the natural viral life cycle and events leading in some cases to malignant transformation (Middleton et al., 2003; Doorbar, 2005).

During the last years this drawback has been overcome by the use of raft cultures which mimic the *in vivo* differentiation process under tissue culture conditions (Chow and Broker, 1997). Transgenic mice were also helpful to understand the oncogenic potential of particular PVs, targeting viral genes to specific tissues and monitoring their pathological outcome (Helfrich et al., 2004; Schaper et al., 2005; Dong et al., 2005). However, the field of *in vivo* models in the context of an organism, i.e. the ordinary history of a PV infection in its natural host, is still underrepresented. The development of such an *in toto* approach would allow us to explore different aspects of carcinogenesis in a complex system of immunocompetent animals.

* Corresponding authors. Angewandte Tumorvirologie, Abteilung Virale Transformationsmechanismen, Deutsches Krebsforschungszentrum, Im Neuenheimer Feld 242, 69120 Heidelberg, Germany. Fax: +49 6221 42 4902.
E-mail address: F.Roesl@DKFZ.de (F. Rösl).

0042-6822/$ - see front matter © 2007 Elsevier Inc. All rights reserved.
doi:10.1016/j.virol.2007.12.012

The soft furred multimammate rat *Mastomys coucha*, earlier assigned to the species *Mastomys natalensis* (Haag et al., 2000), is latently infected with *M. natalensis* papillomavirus (MnPV) (Müller and Gissmann, 1978; Amtmann et al., 1984). These animals develop spontaneously benign skin lesions such as papillomas and keratoacanthomas (Rudolph et al., 1981; Amtmann et al., 1984). The viral DNA is present in an episomal form not only in skin, but also in a whole variety of internal organs, including brain and viral transcription can be detected both in hyperproliferative tissues as well as in tumors (Nafz et al., 2007). Excluding a maternal–foetal transmission route (Nafz et al., 2007), it is assumed that similar to the acquisition of HPV in early infancy (Antonsson et al., 2003), animals get infected very early in their lifespan through microlesions, whereby male animals show a higher incidence of skin tumor formation. The copy numbers of MnPV in healthy skin increases over time and is strongly dependent on the presence of tumors at other sites of the same animal, as determined by hair follicle DNA analysis (Nafz et al., 2007).

Remarkably, these animals also develop condyloma-like lesions at anogenital regions, but the biopsies surprisingly revealed low incidence rates or even a complete absence of MnPV DNA. This raised the question whether a different virus might be etiologically involved. Taking advantage of the modified rolling circle amplification (RCA) method (Rector et al., 2004), we have analysed those lesions for the presence of additional PV types. Here, we have identified and characterised a novel virus that we propose to name *M. coucha* papillomavirus 2 (McPV2) and provide information about the distribution and transcription pattern within its natural host.

Results and discussion

Types of skin lesions in M. coucha

As reported earlier, the *M. coucha* colony at the DKFZ is latently infected with the *M. natalensis* papillomavirus (MnPV) which induces spontaneously papillomas and keratoacanthomas to a frequency of 30–40% at the age of about 1 year (Amtmann et al., 1984; Amtmann and Wayss, 1987). Systematic analyses for the presence and distribution of MnPV in these animals revealed that viral DNA can be detected not only in the skin, but also in internal organs, blood, the lymphatic system and even in brain (Nafz et al., 2007).

Notably, seeking for additional pathological changes, a number of animals also showed condyloma-like lesions at the anus, the penis and the vulva. Considering our colony (currently 380 animals), approximately 7–8% of them develop such lesions at an age of around 8 months. Fig. 1 (panels A and C) depicts two representative examples of the morphology of anogenital lesions exhibiting an exophytic papillary keratotic character. Panel B and D shows a microscopic overview of the corresponding paraffin-embedded tissues after staining with hematoxylin/eosin (HE). Here, characteristic histopathological features of papillomavirus-induced lesions such as pronounced epidermal hyperplasia, papilla-like structures and hyperkeratosis can be detected. Besides these lesions, these two animals also had MnPV positive papilloma-like tumors on the eyelid. In one animal, MnPV DNA could be also detected in apparently healthy skin (Fig. 1E).

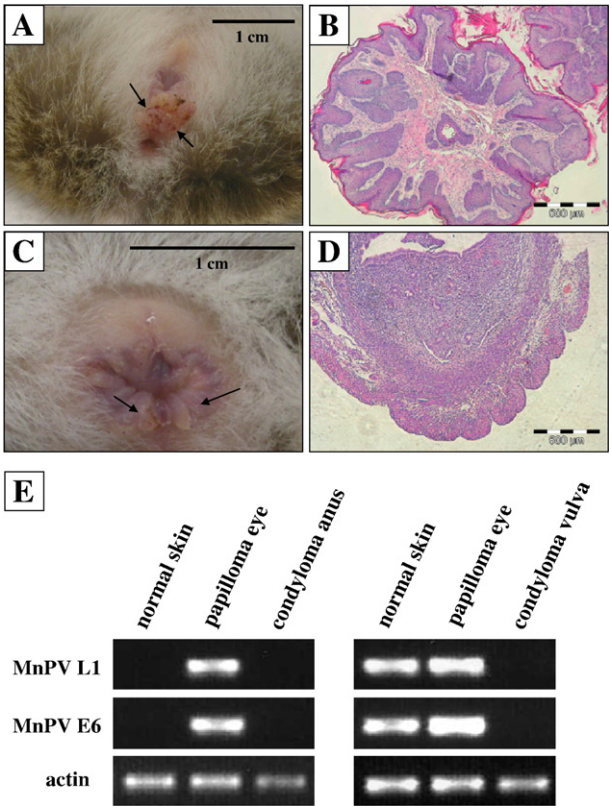

Fig. 1. Examples of McPV2 induced lesions. (A) Anus, (C) vulva. The exophytic condyloma-like growth is indicated by arrows. Right: Microscopic examination of the same lesions after staining with hematoxylin–eosin (HE). (B) Anus. (D) Vulva. Panel E: PCR analysis of DNA extracted from skin, eyelid, anus and vulva using E6/L1 primers of MnPV. To confirm an equal DNA input for the PCR reaction, actin primers were used to amplify an endogenous reference gene.

In contrast, monitoring DNA extracted from the anus or the vulva for the presence of MnPV, none of them were found to be positive, even after application of 30 PCR cycles. To exclude possible structural rearrangement or deletion of the MnPV DNA in these particular lesions, two distal sets of primer were applied, spanning the early and late open reading frame (E6 and L1), respectively. Screening total DNA by PCR analyses, both of them were found to be negative for MnPV (Fig. 1E). However, considering the fact that many species, including humans, chimpanzees, gorillas, cows, dogs or dolphins are the host of multiple different papillomavirus (PV) infections (Antonsson and Hansson, 2002), we next addressed the question whether the failure to detect MnPV could be due to the involvement of other PVs that may infect *M. coucha* at these sites.

Isolation of a novel M. coucha papillomavirus

Initial screening of anogenital lesions with MnPV-specific primers under low stringent hybridization conditions failed to detect any related viral sequences. We therefore used the rolling circle amplification (RCA) technique which selectively amplifies any circular double-stranded DNA without prior knowledge of the viral sequence (Rector et al., 2004). DNA obtained from eye

and anal lesions were cleaved with *Hin*dIII and *Xba*I, two enzymes known to cut MnPV once, as well as with *Pvu*II, having several recognition sites (Tan et al., 1994). Visualizing the bands in an ethidium bromide stained agarose gel, both *Hin*dIII and *Xba*I generated one prominent MnPV unit-length DNA fragment of approximately 7.6 kb in size (Fig. 2, panel A, left), while RCA treated DNA from the anus yielded two bands (indicated by white circles), whose addition resulted to a fragment of approximately 7.5 kb in length (Fig. 2, panel A, right). Hybridization of the filter after Southern blotting with a MnPV-specific probe revealed only positivity of the DNA extracted from the eyelid (see also Fig. 1, panel E), whereas the RCA treated DNA from the anus was negative (Fig. 2, panel B). The two bands obtained after *Hin*dIII digestion were cloned and sequenced. The upper was used for re-probing the filter, demonstrating that there was no cross-hybridization with MnPV (Fig. 2, panel C). Final sequencing of a cloned full-length fragment revealed a completely new

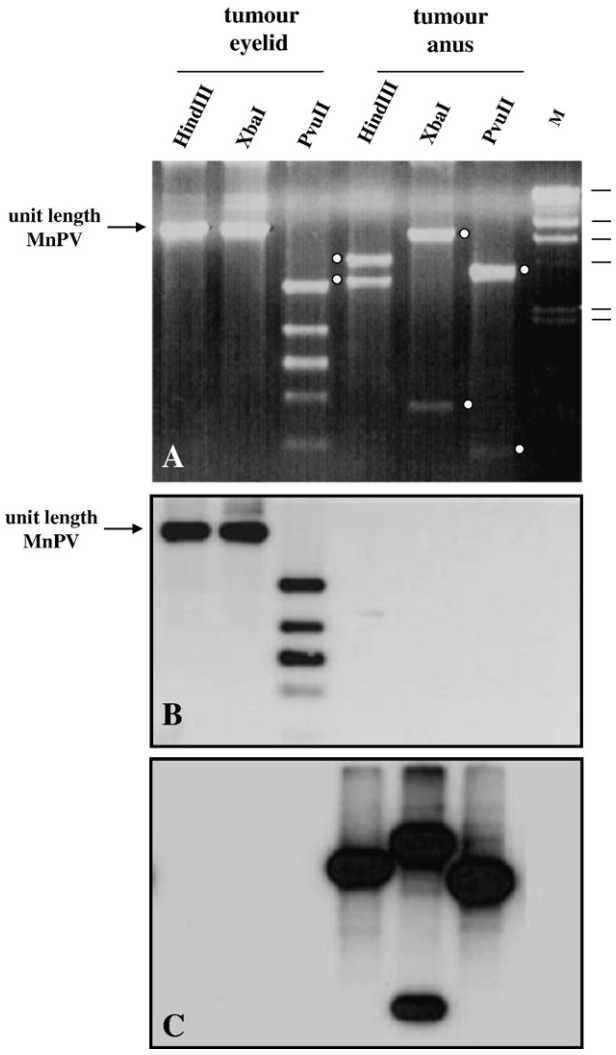

Fig. 2. Rolling circle amplification (RCA) of DNA extracted from eyelid and anal lesions. (A) Ethidiumbromide-stained DNA gel RCA amplicons digested with different restriction enzymes as indicated. *Hin*dIII and *Xba*I are single cutter for MnPV, whereas *Pvu*II is a multi-cutter for MnPV. The white circles highlight the differences in the digestion pattern of the two RCA amplicons obtained after cleavage with the respective restriction enzymes. M: *Hin*dIII digested λ phage DNA as size marker. (B) Southernblot of the DNA gel hybridised with radioactive MnPV-specific probe. Here, no cross-hybridization with DNA amplified from the anal lesion could be discerned. The *Hin*dIII/*Xba*I linearized MnPV DNA is indicated as unit-length MnPV. (C) Same as (B), after re-probing a duplicated filter with the ^{32}P-labeled larger *Hin*dIII fragment (see panel A).

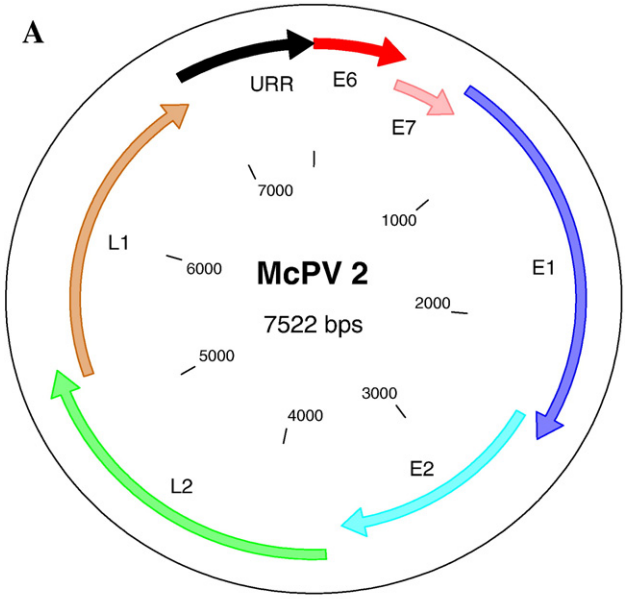

B

ORF of McPV2	genomic location
E6	1-420
E7	420-749
E1	733-2577
E2	2504-3622
L2	3707-5302
L1	5235-6860
URR	6860-7522

C

transcription factors	binding site position
AP-1	7092-7102
AP-1	7343-7350
E2	7229-7244
E2	7285-7299
E2	7462-7575
Sp1	7496-7503

Fig. 3. Genomic organization of *M. coucha* papillomavirus 2 (McPV2). (A) Schematic overview of McPV2. The location and distribution of the early (E) and late (L) open reading frames (ORFs) are indicated. URR = upstream regulatory region. (B) Positions of the start and stop codon of the different ORFs and the corresponding URR. (C) Position of potential binding sites for some important transcription factors (e.g. AP-1, E2, Sp1) within the URR, known to be involved in viral gene regulation. A stringent criterion was applied to predict transcription factor binding sites with MATCH and confirmed by CISTER. Only those factors were chosen with a score above a high cut-off value to minimise false negative and positive outputs.

Table 1
Location and size of the different proteins encoded by McPV2

ORF	nt start position in the genome	Length (aa)	Estimated MW (Da)	Theoretical p*I*
E6	1	139	15,596.2	8.39
E7	420	109	12,079.8	4.52
E1	733	614	69,742.0	5.79
E2	2504	372	42,496.4	8.55
L2	3707	531	56,901.4	4.80
L1	5235	541	61,084.2	8.16

The estimated molecular weight (MW) in Dalton (Da) and the theoretical isoelectric point (pI) is indicated.

papillomavirus (accession number DQ_664501). Since it is now known that the animals belong to the genus *M. coucha* (Haag et al., 2000), the novel virus was designated as *M. coucha* papillomavirus type 2 (McPV2), taking into account that MnPV was the first PV found in this particular host.

Sequence analysis and genome organization

The complete genome of McPV2 (see Fig. 3A, for schematic overview) consists of 7522 bp and shows the basic structure common to all PVes. It encodes for six major open reading frames (ORFs) on one coding strand, with four early (E) and two late (L) proteins. Fig. 3B summarizes the start and the end of the different ORFs. The exact location, length (in amino acids), the estimated molecular weight and the theoretical isoelectric point of the encoded proteins are presented in Table 1. Similar to other skin PVs (for review, see Pfister, 2003), there is no hinge region between E2 and L2 in the McPV2 genome and therefore no ORF encoding for E5-like proteins can be detected (Bravo and Alonso, 2004). McPV2 shares this feature also with closely related PVs that infect skin in rodents (e.g. HaOPV) or MmPV in primates (e.g. HPV4, HPV5, HPV92 or HPV101), carnivores

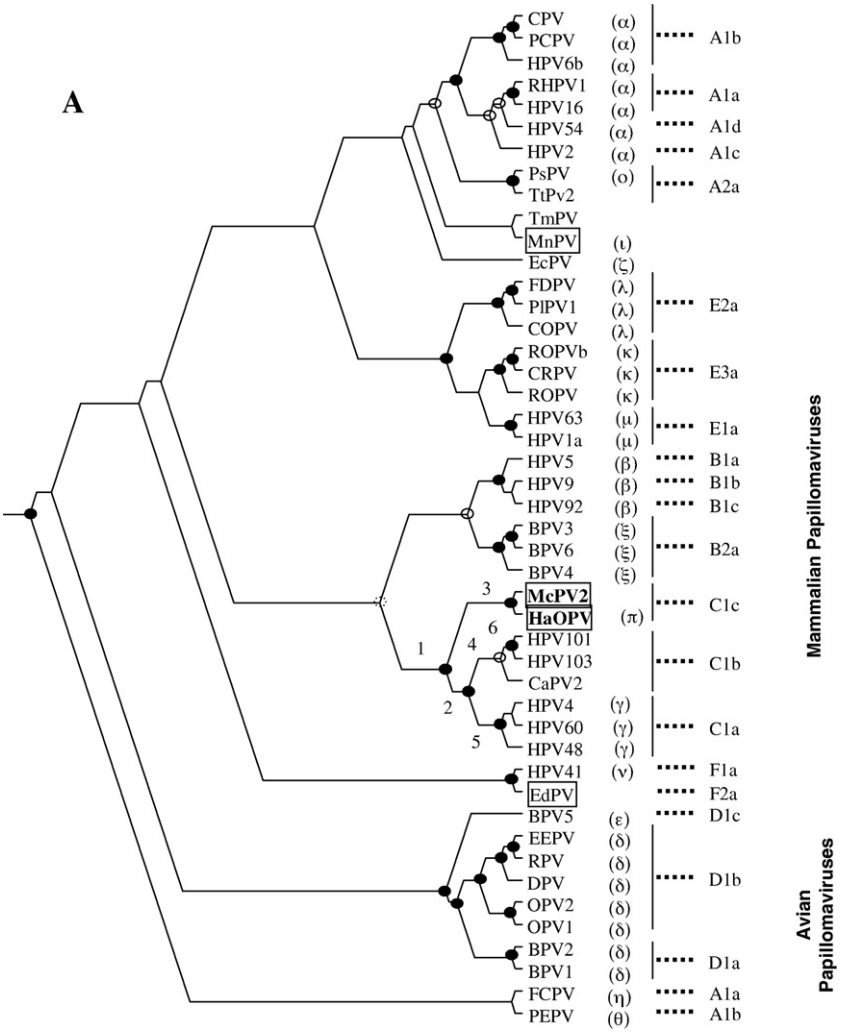

Fig. 4. Phylogenetic analysis of McPV2. (A) Consensus eurogram for the concatenated E1E2L1 sequences from a phylogenetically representative selection of PVs. Viruses infecting rodents are labelled in boxes. Exclusively topology and not distances are depicted. PV classification based on the L1 gene is provided in brackets, while PV classification based on the E1E2 proteins is provided on the right. Black circles, black circumferences and dashed black circumferences label nodes with average support values above 80%, between 60% and 80%, and between 50% and 60%, respectively. PVs infecting rodents are shown in black boxes. McPV2 clusters confidently with the hamster oral PV (HaOPV) and belongs confidently to the mammalian PV supergenus C, following the E1E2-based classification. This supergenus encompasses therefore PV infecting human, dog, hamster and *M. coucha*. (B) Bootstrap support for the different nodes within the Mammalian PV supergenus C, as labelled in the eurogram. Alignment stretches without phylogenetic structure were removed with GBLOCKS, and the result processed with parsimony and distance methods with the PHYLIP software, for Bayesian inference with the BEAST software and for maximum likelihood with the RAxML software. Results are given in percentage after 1000 cycles bootstrap, as posterior probabilities or after 500 cycles bootstrap (maximum likelihood). Distance values for Neighbor-Joining and UPGMA are combined and given under "distances" and support for the Fitch-Margoliash algorithm is given under "f/m". Values are given for both amino acid-based and nucleotide-based (in parentheses) inferences. (C) Evolutionary distances expressed as substitutions per site, measured for the E6, E7, E1, E2, L2 and L1 proteins. Distances were measured between the McPV2 sequence and HaOPV (the closest relative), Mammalian PV C (the clade McPV2 belongs to), Mammalian PV B (the closest clade), the rest of Mammalian PV supergenera and Avian PVs, as defined according to the E1E2-based classification. The evolutionary distances increment in the following order: L1 < E1 < L2 ~ E2 < E6 ~ E7.

B

Node	parsimony	f/m	distances	Bayesian	ML
1	95 (61)	100 (100)	98 (85)	1 (1)	100 (100)
2	- (-)	69 (69)	66 (71)	0.931 (-)	36 (-)
3	100 (100)	100 (100)	100 (100)	1 (1)	100 (100)
4	63 (-)	91 (91)	89 (78)	0.994 (-)	62 (-)
5	98 (99)	96 (96)	98 (100)	1 (1)	100 (100)
6	100 (100)	100 (100)	100 (100)	1 (1)	100 (100)

C

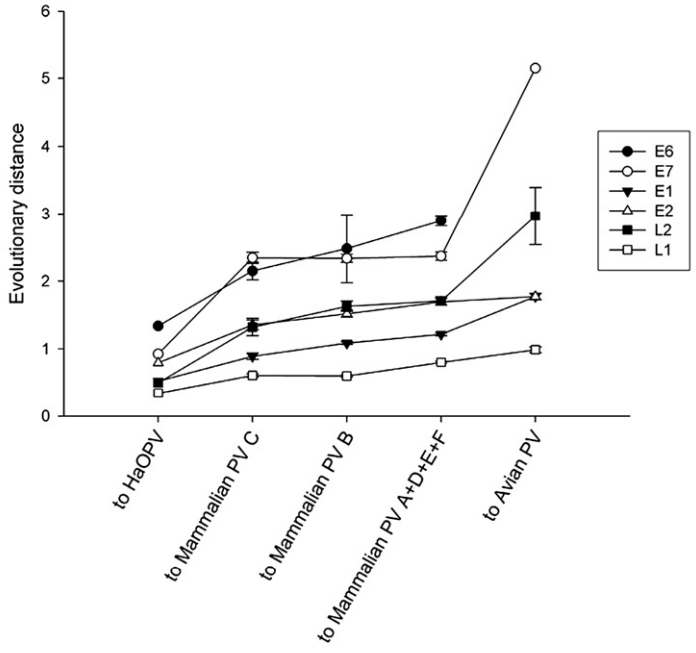

Fig. 4 (*continued*).

(e.g. COPV2) or ruminants (e.g. BPV3). The E1^E4 proteins, are usually expressed after splicing event that links the first five amino acids of E1 to the E4 ORF, nested within E2 on a different reading frame. We were not able to identify any putative E4 ORF, as the two alternative reading frames in E2 were interrupted by several stop codons. Thus, although remnants of the proline-rich stretches that characterise E4 could be identified, we cannot confirm the existence of a true E4 ORF in McPV2. This is not a trivial point, because E1^E4 is the most expressed protein in many HPV infections (Doorbar, 2005; Longworth and Laimins, 2004). Further work characterising the McPV2 transcriptome and a comparison with those in closely related viruses will hopefully provide an explanation to this question.

The McPV2 E6 protein contains two conserved zinc-binding domains, $CX_2C–X_{29}–CX_2C$, separated by 36 amino acids, whereas the E7 contains one such domain. A putative retinoblastoma tumor suppressor-binding domain (DLLCHENLDDPE) is found in the E7 protein. Whether E6 and E7 definitively represent the only viral oncoproteins of McPV, remains to be investigated in further studies. Notably, at least in the case of MnPV, a supportive transforming effect could be confirmed in transgenic mice encoding the E6 oncoprotein under the control of the cytokeratin 14 promoter. Targeting viral gene expression to the basal layer of the skin, we could demonstrate that under conditions where the classical two-stage skin carcinogenesis protocol was applied (Fürstenberger and Kopp-Schneider, 1995), squamous cell carcinomas developed in nearly 100% of the E6 expressing transgenic mice in comparison to only 10% in the non-transgenic littermates (Helfrich et al., 2004). In contrast, corresponding MnPV E7 transgenics were not viable, probably due to the proapoptotic properties of the E7 protein (Nauenburg et al., 2001).

E1 encodes for the largest McPV2 protein of 614 amino acids (Table 1). The ATP-binding site of the ATP-dependent helicase (GPPDTGKS) is conserved in the carboxy-terminal part of E1. The E2 protein can be also divided in an N-terminal *trans*-activation and a C-terminal DNA-binding/dimerization domain separated by a variable hinge region (Hegde and Androphy, 1998). Both the major (L1) and minor (L2) capsid proteins show nuclear localization signals at their carboxyterminus, which are characterised by KR rich sequences. A polyadenylation consensus sequence (AATAAA) of the early viral mRNA transcript is present within the beginning of the L2 ORF (nt 3806 to 3811).

The upstream regulatory region (URR), located between the stop codon of L1 and the first ATG of E6, contains a second polyadenylation site (AATAAA; nt 7017 to 7022) in the 5′ end, probably involved in processing of the late mRNA transcripts. A TATA box can be detected at the 3′ end (nt 7479 to 7482) of the URR, possibly involved in early transcription start. Several

putative transcription factor binding sites (TFBS), which are listed in Fig. 3C, are present. Here, the viral E2 protein plays decisive roles in the viral cycle, since it regulates both viral DNA replication and transcription (for review, see Hegde, 2002). E2 binds as dimers to the cognate palindromic consensus sequence 5′-ACC$(N)_6$GGT-3′ (Androphy et al., 1987), where 3 potential sites can be identified at pos. 7229–7244, 7285–7299 and 7462–7575, respectively. Comparing the URR of its closest relative, the hamster oral PV (HaOPV) (Iwasaki et al., 1997), the distribution pattern of TFBS is highly conserved (data not shown). Furthermore, both regulatory sequences contain a similar palindromic sequence (McPV2 position 7132–7143 and 7151–7163) whose function is still to be defined.

Referring to cellular transcription factors, known to maintain PV gene expression (for review see, Hoppe-Seyler and Butz, 1994; Bernard and Apt, 1994), the McPV2 URR also harbours two potential binding sites for the activator protein-1 (AP-1) (pos. 7092–7102 and 7343–7350). AP-1 has been shown to be indispensable for almost all PV (Sailaja et al., 1999), since deletion or mutation of the corresponding recognition sites completely abrogates transcriptional activity (Butz and Hoppe-Seyler, 1994). In addition, there is also a binding site for the ubiquitous transcription factor Sp1 (pos. 7496–7503) which controls, in conjunction with Sp3, papillomavirus gene expression during differentiation (Apt et al., 1996).

McPV2 phylogeny

Hitherto only five complete genome sequences from PVes that infect rodents are deposited in the databases, corresponding to hamster, harvest mouse, porcupine and *M. natalensis* (now termed *coucha*) (Fig. 4A, black boxes). The finding of a second PV, naturally infecting *M. coucha*, but phylogenetically distant from MnPV suggests that rodents are possibly the host of several types of different PV genera, as in the case of primates, carnivora and cetartiodactyls. For the phylogenetic reconstruction, only the unambiguously codon-aligned sequences of the concatenated E1, E2 and L1 ORFs were used (Fig. 4B). The consensus eurogram for a phylogenetically representative selection of PV sequences is shown (Fig. 4A). Two different PV classification systems based either on the L1 gene (in brackets) (de Villiers et al., 2004) or on the E1E2 proteins (on the right) (Bravo and Alonso, 2007) are provided as a reference. McPV2 clusters confidently with the hamster oral PV HaOPV and both belong with good support to the mammalian PV supergenus C, which encompasses PVes infecting primates, carnivora, artiodactyla and rodentia. The topology of the tree presented here obviously contradicts the extended assumption of PVes having co-evolved parsimoniously with the hosts (Gottschling et al., 2007a). If plain co-evolution had occurred between rodents and PVes that infect rodents, all viruses that infect similar hosts should branch together in the tree, but this is not the case. Thus, MnPV1 is not the closest relative of McPV2, but for both of them, *M. coucha* is the natural host. Besides, the closest relative of porcupine PV EdPV is not a rodent PV but human PV41. Other mechanisms such as recombination (Bravo and Alonso, 2004; Narechania et al., 2005; Varsani et al., 2006), changes in the micro- or macro-ecological conditions (Garcia-Vallve et al., 2006; Narechania et al., 2005) or interspecies transmission (Gottschling et al., 2007a,b) might have also been involved in PV evolution (Gottschling et al., 2007a,b).

We have also analysed the evolutionary distances individually for each ORF, as measured from the McPV2 tip to the different nodes defined with confidence (Fig. 4C). The number of substitutions per site increases in the order L1 < E1 < L2 ~ E2 < E6 ~ E7, which shows that L1 protein is relatively conserved whereas E6 and E7 seem to undergo a rapid evolutionary process. These data support the notion that early proteins have evolved faster than late proteins along the history of PVes, as has already been described for different ORFs and for different PVs (Bravo and Alonso, 2004; Garcia-Vallve et al., 2006; Bravo and Alonso, 2007). The number of substitutions accepted is therefore higher in proteins expressed in the lower layers of the epidermis in the early stage of the infection, and that are potentially exposed to the immune system. On the contrary, the capsid proteins are expressed in the upper layers of the epidermis in the late stages of the infection and might be less exposed to immune surveillance. It is therefore tempting to speculate that at least one of the evolutionary forces that drive the faster evolutionary rates of the oncogenes E6 and E7 is a sort of red Queen race against the immune system.

Presence and distribution of McPV2 in M. coucha

As shown in our previous study, MnPV can also persist in inner organs (Nafz et al., 2007). To monitor whether the novel virus has a similar distribution pattern in its natural host, we autopsied animals and screened for the presence of McPV2 DNA. In order to avoid false positive PCR results, extreme care was taken to exclude cross-contamination. DNA extracted from different specimens were analysed by PCR primers encompassing the E6 ORF McPV2 and compared with the presence of MnPV. Notably, comparing the occurrence of viral DNA (in total, a cohort of 20 animals was investigated), an obvious inverse correlation of MnPV/McPV2 prevalence for internal organs could be observed, with the exception of the skin and benign tumors, where occasionally both viruses can be detected. Fig. 5A illustrates a representative example of an animal that was positive for both viruses. Here, McPV2 was dominant in organs such as liver, kidney, spleen and intestine, whereas MnPV could be only found in the forestomach and in skin (Fig. 5A). This indicates that McPV2 has a similar tropism as previously described for MnPV (Nafz et al., 2007), but a co-existence of both viruses in internal organs seems to be mutually exclusive.

Although MnPV/McPV2 positivity of organs was not accompanied by obvious pathological changes, *M. coucha* may serve as a model to study the question of a broader causal relationship of MnPV/McPV2 in their natural immunocompetent host. It remains to be seen in further experiments whether the presence of MnPV/McPV2 in different organs may also help to understand the involvement of HPV sequences in various other types of human cancer, e.g. in colon (Buyru et al., 2006), lung (Ciotti et al., 2006), esophageal and gastric cancers (Kamangar et al., 2006) as well as in urothelial tumors (Kuwahara et al., 1998).

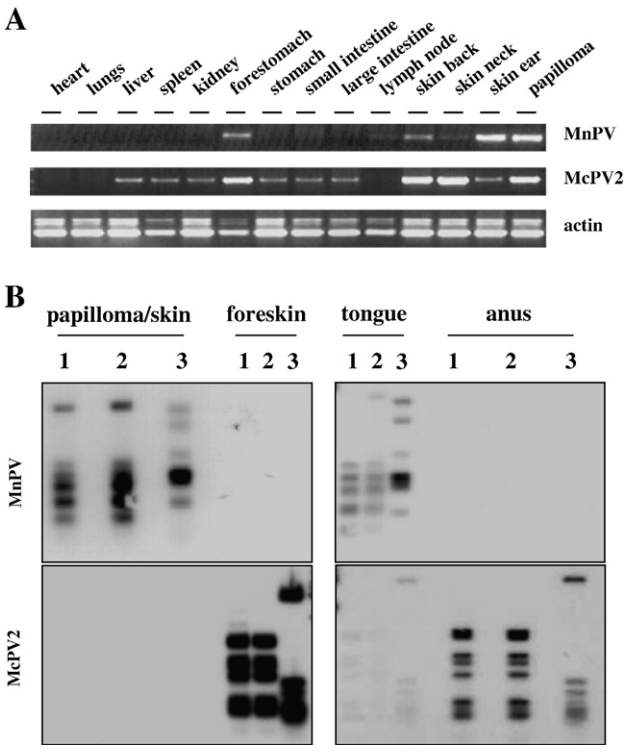

Fig. 5. Prevalence of MnPV and McPV2 DNA within the skin and different lesions. (A) Ethidium bromide-stained gel of PCR analyses to examine the skin and different organs for the presence MnPV and McPV2 DNA. Viral-specific E6 primers and mouse-specific actin primers were used for PCR. The upper band of the actin PCR represents its pseudogene, which was confirmed by DNA sequencing. (B) Southernblot analysis: total genomic DNA obtained from different lesions (skin papilloma, foreskin, tongue and anus) was digested with *Hpa*II (1), *Msp*I (2) and *Hha*I (3) to monitor the methylation status of the viral DNA. The upper filters were hybridized with full-length labelled MnPV, the lower two filters with a labelled McPV2 probe.

The inverse relationship between the prevalence of both viruses can be further substantiated by Southernblot analyses (Fig. 5B). In addition, since it is known that PVes were also targeted by *de novo* methylation that modulates viral transcription (Rösl et al., 1993; Badal et al., 2003), we monitored the epigenetic status of McPV2/MnPV in various lesions (Fig. 5B). DNA extracted from skin, foreskin and tongue was digested with restriction enzymes sensitive or insensitive to CpG methylation in their recognition site. *Msp*I cuts independently of the methylation status, whereas its isoschizomer *Hpa*II and a further enzyme (*Hha*I) cannot cleave when the DNA is methylated. As depicted in Fig. 5B, consecutive hybridization of the same filter with MnPV and McPV2 probes revealed the absence of off-size bands, indicating that the majority of the viral DNA persists in an extrachromosomal state. Moreover, there were no differences between *Hpa*II (lane 1) and *Msp*I (lane 2). Also after digestion with *Hha*I (lane 3), lacking a corresponding isoschizomer, an expected cleavage pattern was revealed. This excludes at least a general *de novo* methylation of both episomal MnPV/McPV2 DNAs, contrasting the situation when PVes were integrated and targeted by the host cell epigenetic machinery (Kim et al., 2003).

Immunostaining and in situ hybridization

To gain insight in the histological features and the distribution of McPV2 and MnPV genomes in anogenital lesions, paraffin embedded normal and pathological vulva tissue was stained with hematoxylin and eosin (HE), while consecutive sections were used for *in situ* hybridization (ISH) with MnPV and McPV2 DNA as specific probes. Fig. 6 shows a representative overview of normal HE stain of the vulva (panel A), being negative for both viral DNAs (panel B and C). Conversely, examining condyloma-like dysplastic tissue, HE staining reveals quite obvious pathological changes, considered to be hallmarks for papillomavirus infection (Lee et al., 1997): epithelial hyperplasia with irregular enlarged, wrinkled hyperchromatic nuclei and koilocytic perinuclear halos (Fig. 6D, see also panel G, indicated by arrows after higher magnification). Notably, using the biotinyltyramide-based ISH technique (Evans et al., 2002), there was no ubiquitous spreading of virus-positive cells within the superficial and intermediate layers (e.g. *stratum spinosum* and the *stratum granulosum*), opposite to what was recently demonstrated for MnPV in skin lesions (Nafz et al., 2007). Instead, only few dysplastic cells (approximately 10%) show strong hybridization signals, indicating that abundant McPV2 replication was taking place in isolated individual cells (Fig. 6, panel E and H). The hybridization pattern was mainly dispersed and not punctuated, which is consistent with previous Southern blot analyses (Fig. 5) showing that the majority of the McPV2 DNA persists in an episomal state (Evans et al., 2002). According to the permissive cycle of papillomaviruses (Doorbar, 2005), no or very weak staining could be discerned in basal cells, since non-differentiated layers regularly harbour low copy numbers of viral DNA. A disproportionate distribution of the viral genomes, varying in their copy number, seems to account for the absence of positive signals in more differentiated regions (Fig. 6, panel E), which are apparently below the detection level achieved by ISH (McNicol and Farquharson, 1997). Indeed, preliminary data suggest that the viral load of McPV2 was consistently lower than in the MnPV-induced lesions. Carrying out the same ISH with parallel tissue samples using MnPV-specific labelled DNA, no signals were obtained (Fig. 6, panel F and I).

Transcriptional analysis

Since under permissive conditions, a target cell may harbour several thousand viral genomes (Doorbar, 2005), analysis of transcriptional activity was done after repeated DNaseI treatments to eliminate contaminating viral DNA. As depicted in Fig. 7, both viruses were transcriptionally active in skin, the corresponding tumors as well as in anogenital lesions, where in this particular specimens co-infection of MnPV and McPV2 occurred. For analyzing viral transcription, primers covering the E6 and L1 ORF of both types were applied for RT-PCR. Actin PCR was performed as a quality control for the DNAse I treated RNA. Taking the intensity of the amplified fragment into account, McPV2 mRNA was less abundantly expressed when the same number of RT-PCR cycles was applied. As already anticipated by ISH (Fig. 6), this was consistent with the notion that MnPV is

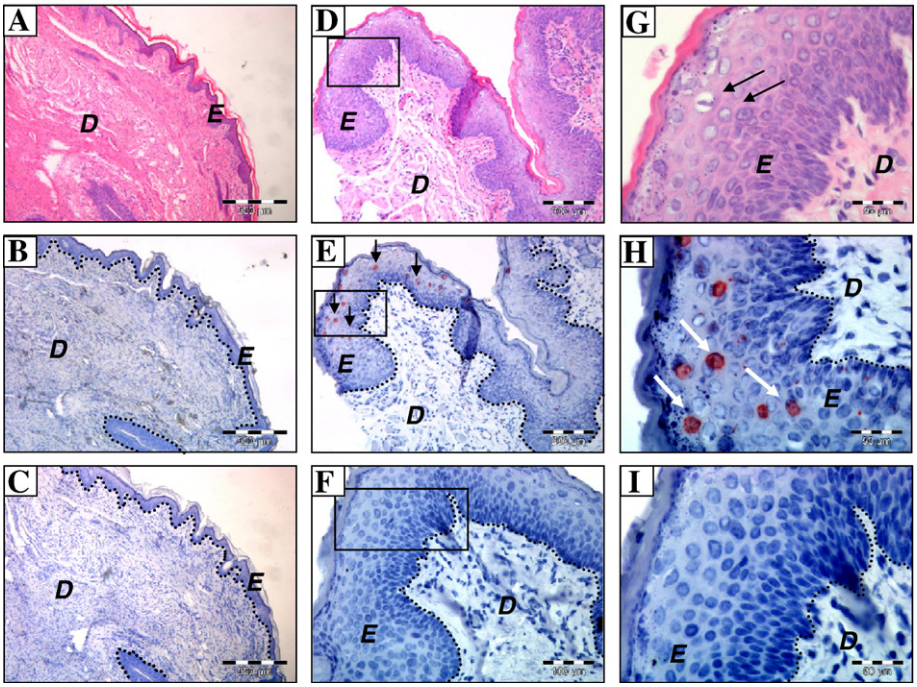

Fig. 6. Histology and *in situ* hybridization (ISH) of normal *versus* dysplastic sections of the vulva. Upper panels: Hematoxylin/Eosin (HE) staining. (A) Normal tissue. (D and G) Dysplastic vulva tissue. The black arrows mark koilocytic atypia within the disorganized morphology of the superficial layer. (B, E, H) Consecutive sections of normal and dysplastic vulva tissue after *in situ* hybridization with McPV2. (C, F, I) Absence of MnPV ISH signals in normal and dysplastic tissue. The dermis (D), the epidermis (E) as well as the scale bars are indicated. The boxed areas in panels D, E and F show which parts are enlarged in panels G, H and I, respectively.

apparently predominant over McPV2 in our *M. coucha* colony. Animal #2 was only expressing the E6 ORF of McPV2, while the corresponding transcript spanning the late region (L1) was absent. Whether this reflects general differences in the early-late switch between the viruses or whether these cells are more prone to undergo malignant transformation remains to be elucidated.

Materials and methods

Animals

M. coucha from the breeding colony of the Deutsches Krebsforschungszentrum were kept under conventional conditions at 21–24 °C and 55% relative humidity and 12–16 air changes/h. The animals were provided with a standardised mouse diet and allowed to drink water *ad libitum*.

Tissue dissection and DNA extraction

To exclude cross contamination from skin to internal organs, scalpels, scissors and forceps were changed after every resection. For DNA extraction, tissue was lysed overnight at 55 °C in DNA lysis buffer (1% SDS, 1 mM EDTA, 100 µg/ml proteinase K, 20 mM Tris/HCl, pH 8) and extracted as described (Sambrook et al., 1989).

Rolling circle amplification (RCA)

Biopsy material was obtained from papillomas or wart-like lesions of different sites from *M. coucha*. To specifically amplify circular double-stranded DNA, multiply-primed RCA using a TempliPhi 100 amplification kit (Amersham Biosciences, Freiburg, Germany) following an optimized protocol (Rector

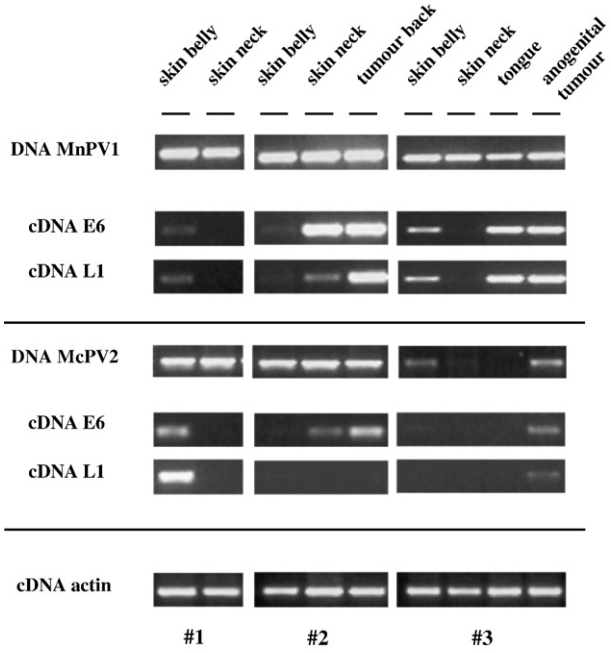

Fig. 7. RT-PCR analysis of various tissues. For RNA extraction, tissue was selected which was positive for MnPV/McPV2 DNA as depicted (DNA PCR with L1 primers). cDNA was analysed by PCR with two different primer pairs representing the early and late ORFs (E6 and L1) of both viruses. β-Actin primers were used to control the integrity of the cellular RNA after repeated DNase treatments.

et al., 2004) was carried out. Briefly, approx. 500 ng of the extracted DNA was denatured in TempliPhi sample buffer (3 min at 95 °C), containing exonuclease-protected random hexamers and then cooled on ice. TempliPhi reaction buffer, containing salts and deoxynucleotides (dNTPs) plus additional 450 μM of dNTPS, and the TempliPhi enzyme mix, containing the ϕ29 DNA polymerase were added to the cooled DNA. Reaction was carried out at 30 °C for 16–18 h in a Thermo-Cycler (Perkin-Elmer). RCA results in exponential, isothermal amplification of the circular DNA and generates linear, double-stranded, high-molecular-weight, tandem-repeated copies of the template DNA (Dean et al., 2001). The reaction was stopped by heating for 10 min at 65 °C and the samples were then kept at 4 °C.

Southern blotting

Southern blotting was performed by standard methods (Sambrook et al., 1989). Briefly, 2.5–5 μg tissue DNA was digested over night (all enzymes indicated were purchased from NEB, Frankfurt, Germany). In the case of RCA, 2 μl of each RCA product was digested with 10 U of different restriction enzymes for 3 h at 37 °C. The DNA was separated in a 1% agarose gel by electrophoresis, blotted on gene screen plus membrane (Perkin Elmer, Rodgau-Jügesheim, Germany) and hybridised with either a MnPV (Amtmann et al., 1984) or McPV2 specific probe. 75–100 ng DNA were labelled with ^{32}P-dCTP using the HexaLabelling kit (MBI Fermentas, St. Leon, Germany). Hybridization was carried out at 37 °C overnight, followed by three washing steps at 68 °C with 2× SSC an 0.1% SDS. The filters were exposed to X-ray films for 8 h to 14 days.

Cloning

Digestion of the RCA amplified DNA of anogenital lesions with *Hin*dIII generated two bands of approx. 3200 and 4300 bp in size, which were gel-purified (QiaexII gel purification kit, Qiagen, Hilden, Germany) and cloned in pBluescript KS vector. After ligation, chemocompetent "One Shot Top10" bacterial cells (Invitrogen, Karlsruhe, Germany) were transformed and plated on Ampicillin/X-Gal-containing agar-plates. White colonies containing the inserts were selected and sequenced. The two fragments encompassed the whole genome of the novel virus. To obtain the complete genome, the RCA DNA was digested with the single cut enzyme *Sal*I, producing one single band which was cloned and re-sequenced at the Sequencing facility of the DKFZ Heidelberg, Germany.

Phylogenetic analysis

A representative selection of sequences from human PVs was chosen, adequately covering all the main subtaxa, as follows: HPV2 [NC_001352], HPV16 [NC_001526], HPV6 [NC_000904], HPV54 [NC_001676]; HPV5 [NC_001531], HPV9 [NC_001596], HPV92 [NC_004500]; HPV4 [NC_001457], HPV48 [NC_001690], HPV60 [NC_001693], HPV101 [NC_008189] and HPV103 [NC_008188]; HPV1 [NC_001356] and HPV 63 [NC_001458]; HPV41 [NC_001354]. Non-human PV complete sequences were included, aiming to cover the widest possible range of host diversity, as follows: PV infecting Primates, *Pan troglodytes* PV [NC_001838] (CPV), *Pan paniscus* PV [NC_006163] (PCPV) and *Macacca mulatta* PV [NC_001678] (RHPV1); PV infecting Rodentia, *M. natalensis* PV [NC_001605] (MnPV), *Erethizon dorsatum* PV (EdPV) [NC_006951] and hamster oral PV (HaOPV) [E15111]; PV infecting Cetartiodactyla, *Phocoena spinipinnis* PV (PsPV) [NC_003348], *Tursiops truncatus* PV2 (TtPV2) [NC_008184], *Bos taurus* PV1 (BPV1) [NC_001522] BPV2 [M20219], BPV3 [AJ620207], BPV4 [X05817], BPV5 [NC_004195], and BPV6 [NC_004711], *Ovis aries* PV1 (OPV1) [NC_001789] and OPV2, *Rangifer tarandus* PV (RPV) [NC_004196], *Alces alces alces* PV (EEPV) [NC_001524] and *Odocoileus virginianus* PV (DPV) [NC_001523]; PV infecting Perissodactyla, *Equus caballus* PV EcPV [NC_004194]; PV infecting Sirenia, *Trichechus manatus latirostris* PV (TmPV) [NC_006563]; PV infecting Carnivora, *Felis catus* PV (FdPV) [AF377865] and *Canis familiaris*, canine oral PV (COPV) [NC_001619] and canine PV2 (CaPV2) [NC_006564]; PV infecting Lagomorpha, *Oryctolagus cuniculus* PV (ROPV) [NC_002232], ROPVb [AJ243287] and *Sylvilagus floridanus* PV (CRPV) [NC_001541]; PV infecting Aves, Passeriformes, *Fringilla coelebs* PV (FcPV) [NC_004068]; PV infecting Aves, Psittaciformes, *Psittacus erithacus* PV (PePV) [NC_003973].

Sequence alignment and phylogenetic analysis

All algorithms were run in the HUSAR environment of the bioinformatics facility of the Deutsches Krebsforschungszentrum. The E1, E2 and L1 ORF were identified (Gottschling et al., 2007a,b), concatenated and aligned at the amino acid level using T-COFFEE, which combines information for both global and local homologies (Notredame et al., 2000). Conserved positions in the original alignment were defined with the GBLOCKS software using non-restringent conditions (freely distributed by Dr. Castresana at http://molevol.ibmb.csic.es) (Castresana, 2000). The refined alignments at the protein level were used for generating codon-alignments at the DNA level, with the PALNAL server (freely distributed by Dr. Suyama at http://coot.embl.de/pal2nal//index.cgi) (Suyama et al., 2006). Both refined alignments, amino acid and codons, were processed for phylogenetic analysis using parsimony (DNAPARS or PROTPARS) and distances (DNADIST or PROTDIST) with the PHYLIP software package (freely distributed by Dr. Felsenstein at http://evolution.genetics.washington.edu/phylip.html) (Felsenstein, 1993). The distance matrices were analysed with FITCH using the Fitch-Margoliash criterion and with NEIGHBOR, under both the Neighbor-Joining (NJ) and Unweighted Pair Group Method with Arithmetic Mean (UPGMA) methods of clustering. The statistical support was assessed by 1000 cycles bootstrapping with SEQBOOT and a consensus tree was computed for each algorithm with CONSENSE. Alignments were also processed for Bayesian Phylogenetic inference with BEAST (freely distributed by Dr. Drummond and Dr. Raumbaut, see http://beast.bio.ed.ac.uk), using a relaxed molecular clock (Drummond et al., 2006): at the codon-aligned

nucleotide level the general time-reversible model was used, partitioning the input into three categories, corresponding to the three codon positions, and generating two runs of 10,000,000 cycles each; at the amino acid level the WAG model was used (Whelan and Goldman, 2001), with four discrete gamma categories, and generating two runs of 1,000,000 cycles each. Maximum Likelihood Analysis was performed with RAxML (freely distributed by Dr. Stamatakis at http://icwww.epfl.ch/~stamatak/index.htm) (Stamatakis et al., 2005): at the codon-aligned level the general time-reversible model with the Γ model of rate heterogeneity was used; at the amino acid level a rtREV substitution model with empirical base frequencies was used (Gottschling et al., 2007a); in both cases a 500 non-parametric bootstrap was used.

Prediction of transcription factor binding sites

Transcription factor binding sites (TFBS) in the genome region between the L1 and the E6 genes of the closely related PVs McPV2 and HaOPV were predicted with MATCH, designed for searching potential binding sites for TFBS nucleotide sequences, using a library of mononucleotide weight matrices from TRANSFAC 9.3 (Wingender et al., 2000). A positive match must have a score higher than or equal to the core similarity cut-off. We have chosen a high cut-off value, designed to minimise both the number of false positives and false negative in the MATCH output. Additionally, we have confirmed the presence of the predicted TFBS in both URR using Cister, an algorithm that uses a technique of posterior decoding based on a hidden Markov model (Frith et al., 2001). Only elements with a posterior probability higher than 0.8 were considered positive in the Cister algorithm. We have chosen an extremely stringent criterion for assessing the presence of TFBS, and only matches appearing in both algorithms were considered true positives.

RNA extraction and Reverse Transcription

Snap frozen tissue was ground with a chilled mortor and pestille, and the tissue powder extracted with Trizol Reagent (Invitrogen, Karlsruhe, Germany) (100 mg tissue/ml Trizol), following the instructions of the manual. RNA was DNase digested with 2–4 µl Turbo DNase (Ambion, Cambridgeshire, UK) prior to reverse transcription and 0.2 µg checked for contaminating viral DNA by the use of virus specific primers (MnPV and McPV L1). Approx. 2 µg of DNase digested RNA was incubated with 3.5 µM Oligo22 dT or 200 ng random primers for 10 min at 42 °C. 0.5 mM dNTPS, single strand buffer, 2.5 mM DTT were added and left for 10 min at 25 °C. After addition of 200 U Superscript II Reverse Transcriptase (Invitrogen), the reaction was incubated at 42 °C for 50 min followed by a final heating to 70 °C for 15 min.

PCR and RT-PCR

100–250 ng genomic DNA or 100 ng cDNA were used for amplification by PCR in a mix containing 1.5 mM $MgCl_2$, 200 µM dNTPs, 0.3 µM of each primer, 1× PCR buffer and 1 Unit recombinant Taq polymerase (Invitrogen, Karlsruhe). PCRs were run in Thermo Cycler MT200 (Biorad, München, Germany) for 25 (DNA) and 28 cycles (cDNA), respectively. The program for all amplifications was: 94 °C 4 min; 25 or 28 cycles of 30 s at 94 °C, 45 s at 58 °C and 30–60 s extension at 72 °C; final extension 10 min 72 °C. Primer sequences for MnPV E6 forward (f): 5′-act cct ttg tgg agc ggc tg-3′, MnPV E6 reverse (r): 5′-caa att ctg cac cgt gcc ctc-3′ (product length: 378 bp); MnPV L1 f: 5′-tct aca ccc gtc att gtc ca-3′, MnPV L1 r: 5′-gcc acg agc tat ctc cac tc-3′(product length: 379 bp); McPV E6 f: 5′-gcg ctt ttt gtg att ctc ct-3′, McPV E6 r: 5′-tgc cag tca tag cct caa ca-3′(product length: 192 bp); McPV L1 f: 5′-tcc caa agt ttc tgg caa tc-3′, McPV L1 r: 5′-caa aca gct cat tgc tcc aa-3′ (product length: 817 bp), actin f: 5′-acc cac act gtg ccc atc tac ga-3′, actin r: 5′-ctt gct gat cca cat ctg ctg ga-3′.

Histology

Tissue samples were fixed in formalin and subsequently embedded in paraffin. 2–5 µm thick sections were taken from the paraffin blocks, placed on coated slides and fixed overnight at 56 °C. The first cut of each specimen was stained with hematoxylin and eosin in order to illustrate histopathological changes, consecutive sections were used for *in situ* hybridization (ISH) to analyze the presence of viral DNA.

In situ hybridization

Full-length MnPV and McPV2 genomes were cloned in pUC19 plasmids and biotin-labelled by nick-translation (Roche, Mannheim, Germany). 5-µm sections of paraffin-embedded tissue were fixed at 56 °C on 3-aminopropyltriethoxysilane (APES) coated slides overnight and deparaffinized by incubating twice in xylene followed by rehydration in a graded ethanol series and water. Specimens were boiled in sodium citrate buffer for 10 min in a microwave oven and digested with pepsin (8 µg/ml 0.1 N HCl) for 30–40 min at 37 °C. To extinguish residual peroxidase activity, the slides were incubated in 3% H_2O_2 solution for 10 min and afterwards treated with 4% paraformaldehyde for 30 min. For hybridization, the appropriate probe was added in a concentration of 500 ng/ml in hybridization buffer (50% formamide, 2× SSC, 1 mg/ml sonificated salmon sperm DNA, 0.05 M NaH_2PO_4/Na_2HPO_4, 1 mM EDTA) and the slides were heated at 98 °C for 8 min followed by incubation at 42 °C in a moist chamber for 16 h. The slides were then stringently washed in 2–0.1× SSC/0.05% Tween20 from 37 °C to 55 °C. Following the instruction of the TSA amplification kit (Perkin Elmer), slides were incubated with a streptavidin–horseradish peroxidase conjugate (dilution 1:500) and the signal was amplified with biotinyl-tyramide (dilution 1:50). Viral DNA was then visualised by a chromogen reaction using 3-amino-9-ethylcarbazole (AEC; DakoCytomation) and the tissue was counterstained with hematoxylin.

Acknowledgments

The authors are grateful to Andreas Hunziker (Oligosynthesis/Sequencing unit, DKFZ) for sequencing, Prof. Harald zur

Hausen for critical reading the manuscript and Dr. Bladimiro Orozco Rincon for his help in computer work. IGB is supported by the Volkswagen Foundation under the initiative "Evolutionary Biology".

References

Akgül, B., Cooke, J.C., Storey, A., 2006. HPV-associated skin disease. J. Pathol. 208, 165–175.

Amtmann, E., Wayss, K., 1987. The *Mastomys natalensis* Papillomavirus. In: Salzman, Norman P., Howley, Peter H. (Eds.), The Papovaviridae. Plenum Publishing Corporation, pp. 187–198.

Amtmann, E., Volm, M., Wayss, K., 1984. Tumour induction in the rodent *Mastomys natalensis* by activation of endogenous papilloma virus genomes. Nature 308, 291–292.

Androphy, E.J., Lowy, D.R., Schiller, J.T., 1987. Bovine papillomavirus E2 trans-activating gene product binds to specific sites in papillomavirus DNA. Nature 325, 70–73.

Antonsson, A., Hansson, B.G., 2002. Healthy skin of many animal species harbors papillomaviruses which are closely related to their human counterparts. J. Virol. 76, 12537–12542.

Antonsson, A., Karanfilovska, S., Lindqvist, P.G., Hansson, B.G., 2003. General acquisition of human papillomavirus infections of skin occurs in early infancy. J. Clin. Microbiol. 41, 2509–2514.

Apt, D., Watts, R.M., Suske, G., Bernard, H.U., 1996. High Sp1/Sp3 ratios in epithelial cells during epithelial differentiation and cellular transformation correlate with the activation of the HPV-16 promoter. Virology 224, 281–291.

Badal, V.L., Chuang, S.H., Tan, E.H.H., Bahal, S., Villa, L.L., Wheeler, C.M., Li, B.F.L., Bernard, H.U., 2003. CpG methylation of human papillomavirus type 16 DNA in cervical cancer cell lines and in clinical specimens: genomic hypomethylation correlates with carcinogenic progression. J. Virol. 77, 6227–6234.

Bernard, H.U., Apt, D., 1994. Transcriptional control and cell type specificity of HPV gene expression. Arch. Dermatol. 130, 210–215.

Bravo, I.G., Alonso, A., 2004. Mucosal human papillomaviruses encode four different E5 proteins whose chemistry and phylogeny correlate with malignant or benign growth. J. Virol. 78, 13613–13626.

Bravo, I.G., Alonso, A., 2007. Phylogeny and evolution of papillomaviruses based on the E1 and E2 proteins. Virus Genes 34, 249–262.

Butz, K., Hoppe-Seyler, F., 1994. Transcriptional control of human papillomavirus (HPV) oncogene expression: composition of the HPV type 18 upstream regulatory region. J. Virol. 67, 6476–6486.

Buyru, N., Tezol, A., Dalay, N., 2006. Coexistence of K-ras mutations and HPV infection in colon cancer. BMC Cancer 6, 1–5.

Castresana, J., 2000. Selection of conserved blocks from multiple alignments for their use in phylogenetic analysis. Mol. Biol. Evol. 17, 540–552.

Chow, L.T., Broker, T.R., 1997. In vitro experimental systems for HPV: epithelial raft cultures for investigations of viral reproduction and pathogenesis and for genetic analyses of viral proteins and regulatory sequences. Clin. Dermatol. 15, 217–227.

Ciotti, M., Giuliani, L., Ambrogi, V., Ronci, C., Benedetto, A., Mineo, T.C., Syrjanen, K., Favalli, C., 2006. Detection and expression of human papillomavirus oncogenes in non-small cell lung cancer. Oncol. Rep. 16, 183–189.

de Villiers, E.M., Fauquet, C., Broker, T.R., Bernard, H.U., zur Hausen, H., 2004. Classification of papillomaviruses. Virology 324, 17–27.

Dean, F.B., Nelson, J.R., Gesler, T.L., Lasken, R.S., 2001. Rapid amplification of plasmid and phage DNA using phi29 DNA polymerase and multiply-primed rolling circle amplification. Genome Res. 11, 1095–1099.

Dong, W., Kloz, U., Accardi, R., Caldeira, S., Tong, W.M., Wang, Z.Q., Jansen, L., Durst, M., Sylla, B.S., Gissmann, L., Tommasino, M., 2005. Skin hyperproliferation and susceptibility to chemical carcinogenesis in transgenic mice expressing E6 and E7 of human papillomavirus type 38. J. Virol. 79, 14899–14908.

Doorbar, J., 2005. The papillomavirus life cycle. J. Clin. Virol. 32 (Suppl 1), 7–15.

Drummond, A.J., Ho, S.Y., Phillips, M.J., Rambaut, A., 2006. Relaxed phylogenetics and dating with confidence. PLoS Biol. 4, 699–710.

Evans, M.F., Mount, S.L., Beatty, B.G., Cooper, K., 2002. Biotinyl-tyramide-based in situ hybridization signal patterns distinguish human papillomavirus type and grade of cervical intraepithelial neoplasia. Mod. Path. 15, 1339–1347.

Felsenstein, J., 1993. PHYLIP (Phylogeny Inference Package) version 3.5c. Distributed by the author. Department of Genetics, University of Washington, Seattle. http://evolution.genetics.washington.edu/phylip.html.

Frith, M.C., Hansen, U., Weng, Z., 2001. Detection of *cis*-element clusters in higher eukaryotic DNA. Bioinformatics 17, 878–889.

Fürstenberger, G., Kopp-Schneider, A., 1995. Malignant progression of papillomas induced by the initiation–promotion protocol in NMRI mouse skin. Carcinogenesis 16, 61–69.

Garcia-Vallve, S., Iglesias-Rozas, J.R., Alonso, A., Bravo, I.G., 2006. Different papillomaviruses have different repertoires of transcription factor binding sites: convergence and divergence in the upstream regulatory region. BMC Evol. Biol. 6, 1–14.

Gottschling, M., Stamatakis, A., Nindl, I., Stockfleth, E., Alonso, A., Bravo, I.G., 2007a. Multiple evolutionary mechanisms drive papillomavirus diversification. Mol. Biol. Evol. 24, 1242–1258.

Gottschling, M., Köhler, A., Stockfleth, E., Nindl, I., 2007b. Phylogenetic analysis of beta-papillomaviruses as inferred from nucleotide and amino acid sequence data. Mol. Phylogenet. Evol. 42, 213–222.

Haag, A., Wayss, K., Rommelaere, J., Cornelis, J.J., 2000. Experimentally induced infection with autonomous parvoviruses, minute virus of mice and H-1, in the African multimammate mouse (*Mastomys coucha*). Comp. Med. 50, 613–621.

Hegde, R.S., 2002. The papillomavirus E2 proteins: structure, function and biology. Annu. Rev. Biophys. Biomol. Struct. 31, 343–360.

Hegde, R.S., Androphy, E.J., 1998. Crystal structure of the E2 DNA-binding domain from human papillomavirus type 16: implications for its DNA binding site selection mechanism. J. Mol. Biol. 284, 1479–1489.

Helfrich, I., Chen, M., Schmidt, R., Furstenberger, G., Kopp-Schneider, A., Trick, D., Gröne, H.J., zur Hausen, H., Rösl, F., 2004. Increased incidence of squamous cell carcinomas in *Mastomys natalensis* papillomavirus E6 transgenic mice during two-stage skin carcinogenesis. J. Virol. 78, 4797–4805.

Hoppe-Seyler, F., Butz, K., 1994. Cellular control of human papillomavirus oncogene transcription. Mol. Carcinog. 10, 134–141.

Iwasaki, T., Maeda, H., Kameyama, Y., Moriyama, M., Kanai, S., Kurata, T., 1997. Presence of a novel hamster oral papillomavirus in dysplastic lesions of hamster lingual mucosa induced by application of dimethylbenzanthracene and excisional wounding: molecular cloning and complete nucleotide sequence. J. Gen. Virol. 78, 1087–1093.

Kamangar, F., Qiao, Y.L., Schiller, J.T., Dawsey, S.M., Fears, T., Sun, X.D., Abnet, C.C., Zhao, P., Taylor, P.R., Mark, S.D., 2006. Human papillomavirus serology and the risk of esophageal and gastric cancers: results from a cohort in a high-risk region in China. Int. J. Cancer 119, 579–584.

Kim, K., Garner-Hamrick, P.A., Fisher, C., Lee, D., Lambert, P.F., 2003. Methylation patterns of papillomavirus DNA, its influence on E2 function, and implications in viral infection. J. Virol. 77, 12450–12459.

Kuwahara, M., Fujisaki, N., Kagawa, S., Furihata, M., Ohtsuki, Y., 1998. Determination of p53 protein and high-risk human papillomavirus DNA in carcinomas of the renal pelvis and ureter. Int. J. Mol. Med. 1, 703–707.

Lee, K.R., Minter, L.J., Crum, C.P., 1997. Koilocytic atypia in Papanicolaou smear. Cancer 81, 10–15.

Longworth, M.S., Laimins, L.A., 2004. Pathogenesis of human papillomaviruses in differentiating epithelia. Microbiol. Mol. Biol. Rev. 68, 362–372.

Majewski, S., Jablonska, S., 2006. Current views on the role of human papillomaviruses in cutaneous oncogenesis. Int. J. Dermatol. 45, 192–196.

McNicol, A.M., Farquharson, M.A., 1997. In situ hybridization and its diagnostic applications in pathology. J. Pathol. 182, 250–261.

Middleton, K., Peh, W., Southern, S., Griffin, H., Sotlar, K., Nakahara, T., El Sherif, A., Morris, L., Seth, R., Hibma, M., Jenkins, D., Lambert, P., Coleman, N., Doorbar, J., 2003. Organization of human papillomavirus productive cycle during neoplastic progression provides a basis for selection of diagnostic markers. J. Virol. 77, 10186–10201.

Müller, H., Gissmann, L., 1978. *Mastomys natalensis* papilloma virus (MnPV), the causative agent of epithelial proliferations: characterization of the virus particle. J. Gen. Virol. 41, 315–323.

Nafz, J., Köhler, A., Ohnesorge, M., Nindl, I., Stockfleth, E., Rösl, F., 2007. Persistence of *Mastomys natalensis* papillomavirus in multiple organs identifies new targets for infection. J. Gen. Virol. 88, 2670–2678.

Narechania, A., Chen, Z., DeSalle, R., Burk, R.D., 2005. Phylogenetic incongruence among oncogenic genital alpha human papillomaviruses. J. Virol. 79, 15503–15510.

Nauenburg, S., Zwerschke, W., Jansen-Dürr, P., 2001. Induction of apoptosis in cervical carcinoma cells by peptide aptamers that bind to the HPV-16 E7 oncoprotein. FASEB J. 15, 592–594.

Nindl, I., Gottschling, M., Stockfleth, E., 2007. Human papillomaviruses and non-melanoma skin cancer: basic virology and clinical manifestations. Dis. Markers 23, 247–259.

Notredame, C., Higgins, D., Heringa, J., 2000. T-Coffee: a novel method for multiple sequence alignments. J. Mol. Biol. 302, 205–217.

Pfister, H., 2003. Chapter 8: human papillomavirus and skin cancer. J. Natl. Cancer Inst. 52–56.

Rector, A., Tachezy, R., van Ranst, M., 2004. A sequence-independent strategy for detection and cloning of circular DNA virus genomes by using multiply primed rolling-circle amplification. J. Virol. 78, 4993–4998.

Rösl, F., Arab, A., Klevenz, B., zur Hausen, H., 1993. The effect of DNA methylation on gene regulation of human papillomaviruses. J. Gen. Virol. 74, 791–801.

Rudolph, R.L., Muller, H., Reinacher, M., Thiel, W., 1981. Morphology of experimentally induced so-called keratoacanthomas and squamous cell carcinomas in 2 inbred-lines of *Mastomys natalensis*. J. Comp. Pathol. 91, 123–134.

Sambrook, J., Fritsch, E.F., Maniatis, T., 1989. Molecular Cloning: A Laboratory Manual. Cold Spring Harbor Laboratory, Cold Spring Harbor, NY.

Sailaja, G., Watts, R.M., Bernard, H.U., 1999. Many different papillomaviruses have low transcriptional activity in spite of strong epithelial specific enhancers. J. Gen. Virol. 80, 1715–1724.

Schaper, I.D., Marcuzzi, G.P., Weissenborn, S.J., Kasper, H.U., Dries, V., Smyth, N., Fuchs, P., Pfister, H., 2005. Development of skin tumors in mice transgenic for early genes of human papillomavirus type 8. Cancer Res. 65, 1394–1400.

Suyama, M., Torrents, D., Bork, P., 2006. PAL2NAL: robust conversion of protein sequence alignments into the corresponding codon alignments. Nucleic Acids Res. 34, W609–W612.

Stamatakis, A., Ludwig, T., Meier, H., 2005. RAxML-III: a fast program for maximum likelihood-based inference of large phylogenetic trees. Bioinformatics 21, 456–463.

Tan, C.H., Tachezy, R., van Ranst, M., Chan, S.Y., Bernard, H.U., Burk, R.D., 1994. The *Mastomys natalensis* papillomavirus: nucleotide sequence, genome organization, and phylogenetic relationship of a rodent papillomavirus involved in tumorigenesis of cutaneous epithelia. Virology 198, 534–541.

Varsani, A., Williamson, A.L., Jaffer, M.A., Rybicki, E.P., 2006. A deletion and point mutation study of the human papillomavirus type 16 major capsid gene. Virus Res. 122, 154–163.

Whelan, S., Goldman, N., 2001. A general empirical model of protein evolution derived from multiple protein families using a maximum-likelihood approach. Mol. Biol. Evol. 18, 691–699.

Wingender, E., Chen, X., Hehl, R., Karas, H., Liebich, I., Matys, V., Meinhardt, T., Pruss, M., Reuter, I., Schacherer, F., 2000. TRANSFAC: an integrated system for gene expression regulation. Nucleic Acids Res. 28, 316–319.

Woodman, C.B., Collins, S.I., Young, L.S., 2007. The natural history of cervical HPV infection: unresolved issues. Nat. Rev., Cancer 7, 11–22.

zur Hausen, H., 2002. Papillomaviruses and cancer: from basic studies to clinical application. Nat. Rev., Cancer 2, 342–350.